

Energy Dependence of the Latitude of the 1-25 KeV Ion Isotropy Boundary

Eric F. Donovan, Brian J. Jackel, Robert J. Strangeway, and David M. Klumpar

Department of Physics and Astronomy, University of Calgary, Alberta, Canada

Institute of Geophysics and Planetary Physics, UCLA, Los Angeles, California, USA

Physics Department SSEL, Montana State University, Bozeman, Montana, USA

Received: 10.1.2002 – Accepted: 15.5.2002

1 Introduction

Precipitating magnetospheric protons undergo charge exchange collisions with atmospheric atoms, ions, and molecules. The newly formed hydrogen atoms are left in excited states, and upon relaxation emit photons characteristic of hydrogen electronic transitions (for example, the Balmer α , β and Lyman α lines). The resulting emissions comprise the *proton aurora*. On the night-side, the proton aurora is understood to result from precipitation of central plasma sheet (CPS) protons. These night-side emissions are diffuse and form an oval, statistically being at higher magnetic latitudes at dusk and dawn than at midnight (Donovan et al., 2002). The proton aurora have been observed from the ground using photometers, spectrographs, all-sky imagers, and more recently from space with the IMAGE spacecraft. Figure 1 is a keogram of proton auroral Balmer β intensities from the CANOPUS Gillam meridian scanning photometer (MSP).

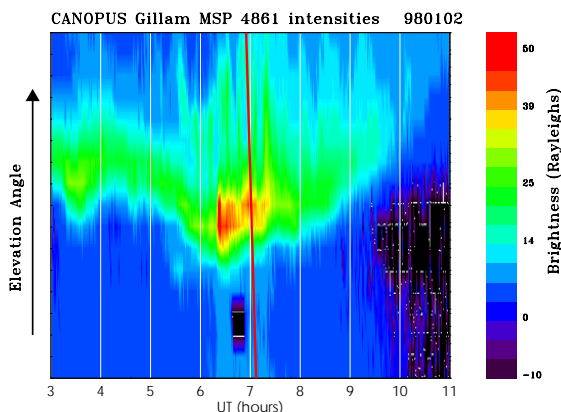


Fig. 1. Keogram of hydrogen Balmer β (486 nm) data from the CANOPUS Gillam MSP for eight hours bracketing the time of a FAST satellite overflight (indicated by the red line around 0700 UT).

Correspondence to: E.F. Donovan

On the basis of satellite and rocket overflights of the proton auroral oval, it has been established that the precipitating protons have energies characteristic of CPS ions (ie., from <1 KeV to upwards of 100 KeV). The proton distribution functions are more or less isotropic outside of an empty upgoing loss cone, and this isotropy exists across a wide range of energies. The full downgoing loss cone is consistent with scattering processes, rather than field-aligned acceleration, being the direct cause of the precipitation. Equatorward of the proton aurora, both the downgoing and upgoing proton loss cones are virtually empty, a distribution characteristic of bounce trapped particles. The transition between the full and empty downgoing loss cone is called the isotropy boundary (IB). The latitude of the IB is, in general, a function of magnetic local time, particle energy, and the state of the magnetosphere. The equatorward boundary of the IB typically corresponds to both the equatorward boundary of the proton aurora and the b2i boundary identified routinely in DMSP ion data (Newell et al., 1996, 1998; Donovan et al., 2002).

The mechanism responsible for scattering most likely operates near the magnetospheric equatorial plane, and is almost certainly due to either one or both of wave-particle interactions and *slight* breaking of the first adiabatic invariant due to the relatively tightly curved field lines in the vicinity of the neutral sheet. On the basis of simulations of protons moving in realistic magnetospheric magnetic fields, Sergeev and Tsyganenko (1982) determined that if the ratio of radius of curvature of field lines in the neutral sheet (where, presumably, the gyroradius is largest and the field line curvature is tightest) to the local proton gyroradius was smaller than about 8, then there would be enough scattering to just fill the loss cone. If this *field line curvature* (herein FLC) mechanism is the primary source of pitch angle scattering, then the IB marks the transition across which the so-called κ -parameter (see Büchner and Zelenyi (1987)) goes from greater than, to less than, $\sim \sqrt{8}$. The κ -parameter depends on particle energy (through the gyroradius) and hence the location of the IB surface will depend on energy. The scattering condition (ie., $\kappa \gtrsim 3$) will be satisfied closer to the Earth for

more energetic protons than for less energetic protons. This would mean that if the scattering is caused by FLC, then the IB in the top-side ionosphere would be more equatorward for higher energy particles. *In situ* observations of variations in IB latitude with energy are consistent with the scattering being caused by FLC, at least for protons with energies greater than 30 KeV (Imhoff et al., 1977; Sergeev et al., 1982).

Based on the above, it is now generally accepted that the primary cause of proton auroral precipitation is pitch angle scattering of CPS protons due to FLC. For example, in recent modelling work, Wanliss et al. (2000) have used the equatorward edge of the proton aurora to identify field lines that thread the CPS in the region where $\kappa \sim 3$ for protons with energies characteristic of the precipitating particles. However, the bulk of the energy flux responsible for the proton aurora, at least during quiet or moderately active times, is carried by protons with energies between 1 and 30 KeV. Thus, the existing observational evidence of FLC induced scattering strictly applies only to protons outside of the energy range relevant to the proton aurora. In this paper, we use Fast Auroral Snapshot Explorer (FAST) electrostatic analyzer (ESA) ion data to explore the energy dependence of the latitude of the IB in the energy range relevant to the bulk of the night-side proton auroral precipitation. We present a description of the FAST ESA instrument, show results from a FAST overflight of the Gillam MSP, demonstrate our use of the FAST ESA data to determine the IB latitude for a particular energy range, and finally give the results of a preliminary statistical study of the energy dependence of the IB latitude.

2 The FAST ESA Instrument

FAST is a NASA Small Explorer program mission with a focus on high spatial and temporal resolution measurements of charged particles and magnetic and electric fields in the low altitude auroral acceleration region (Carlson et al., 1998). FAST was launched on August 21, 1996 into an 83° inclination elliptical orbit of 350 km by 4175 km. These orbital elements place the satellite in the auroral oval four times per orbit (approximately 11 orbits per day) over a wide range of altitudes, local times, and seasons as the orbital motion evolves through time. The instrument complement includes 16 “top-hat” electrostatic analysers (herein collectively referred to as ESA) which provide measurements of charged particle pitch angle distributions (Carlson et al., 1998).

Each ESA analyzer has a 180° field-of-view lying in the satellite spin plane, which is typically aligned within 6° of the geomagnetic field (in the auroral zones). Twelve of the sixteen are operated as fast electron spectrographs to obtain ultrahigh time resolution (1.7 ms) electron measurements in 16-pitch angle bins. The other four ESAs are operated in opposing pairs as ion and electron spectrometers to make high resolution distribution measurements instantaneously covering all pitch angles with 32 pitch angle bins every 70 ms. The spectrometers have deflection plates to automatically steer their fields of views to track the measured magnetic field di-

rection. The measurement energy range is 4 eV to 30 keV for electrons and 3 eV to 25 keV for ions. The FAST data used in this study comes exclusively from the publicly available ESA ion data provided by CDAWeb.

FAST overflew the Gillam MSP at the time indicated by the red curve in Figure 1. In Figure 2, we present some details of the FAST ESA ion data. Note the correspondence between the profiles of downgoing integrated energy flux and the proton auroral intensity (top panel), the fact that the optical proton aurora is in a region that maps to the CPS (>5 KeV ion population in the spectrograph in the bottom panel), and that the equatorward boundary of the proton aurora is co-located with the isotropy boundary.

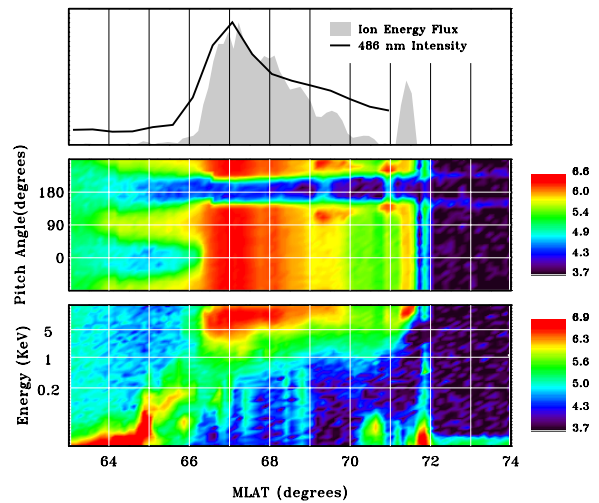


Fig. 2. Summary of FAST ESA ion data from an overflight of the Gillam MSP. Top: integrated downward ion energy flux measured by FAST (shaded) and 486.1 nm intensity observed by the Gillam MSP (line). Both curves have been autoscaled. The MSP intensity profile is an average of several scans obtained during the FAST overflight and we have presumed an emission altitude of 110 km. Middle: FAST ESA ion integrated energy flux as a function (note the polar cap boundary, empty upgoing loss cone throughout the CPS, and empty downgoing loss cone in the inner CPS). Bottom: FAST ESA ion differential energy spectrogram.

3 The Isotropy Boundary (IB)

As stated in the introduction, the IB is the equatorward boundary of significant ion precipitation, and marks the transition between full and empty downgoing loss cones. For the FAST data shown in Figure 2 this occurs at an invariant latitude of roughly 66.5° . In Figure 3, we show the integrated ion energy flux for four successive satellite spins that bracket this transition. The isotropy boundary spans roughly 0.5° degrees latitude, consistent with the observations of Sergeev and Gvozdevsky (1995). There are contributions to the integrated energy flux from ions with energies ranging from < 1 KeV to the instrument limit of 25 KeV. In Figure 4, we show the parallel (**B** field aligned) and orthogonal differential energy fluxes of 25 KeV ions and the ratio of the two quantities for another FAST transit of the evening sector auroral oval.

We refer to the ratio of perpendicular to parallel differential energy flux as the *isotropy ratio*. The isotropy ratio is roughly 1 throughout most of the CPS and increases rapidly near the inner edge of the CPS. This general behaviour holds for most particle energies and local times.

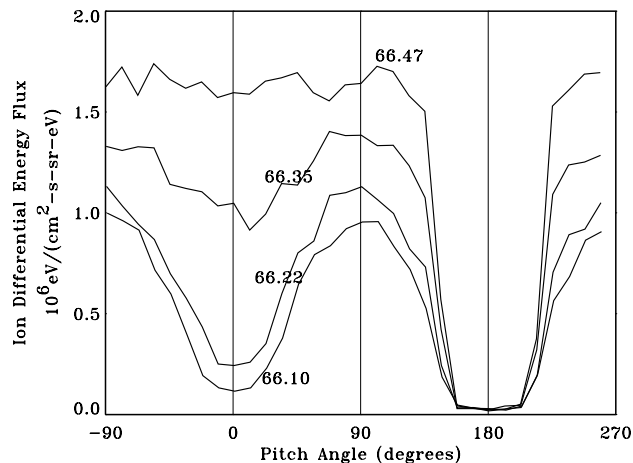


Fig. 3. The Isotropy Boundary (IB): FAST ESA ion differential energy flux (1-30 KeV), showing the transition between the full and empty downgoing loss cones. These observations are from the same overflight during which the data shown in Figures 1 and 2 were obtained. Numbers by each curve indicate the invariant latitudes.

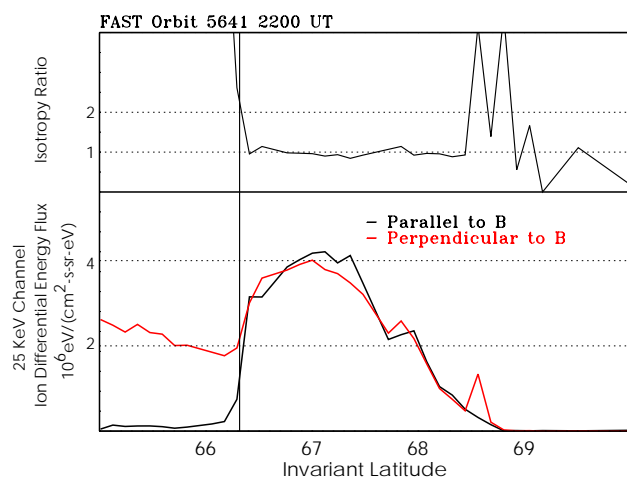


Fig. 4. Top: isotropy ratio of perpendicular to parallel differential energy fluxes for 25 KeV ions obtained during a transit of the evening sector auroral oval (FAST orbit 5641). Bottom: perpendicular and parallel differential energy fluxes of 25 KeV ions. Note that the IB is the location where the isotropy ratio becomes larger than 1, near the equatorward edge of field lines threading the CPS.

4 IB Latitude Energy Dependence

The IB can be viewed as a transition in either the integrated energy flux, or the differential energy flux at a particular energy. In other words, we can think of the 25 KeV ion IB, the 5 KeV ion IB, the 400 KeV electron IB, and so on. If the scattering process that fills the loss cone is energy dependent, then the IB will be at different latitudes for different energies and different particles (eg. Imhoff et al., 1977). In Figure 5 we show the isotropy ratio for five energies spanning the 1-25 KeV range, for an evening sector auroral oval transit. In this pass, IBs for successively higher energy ions are at progressively lower latitudes, consistent with scattering due to FLC.

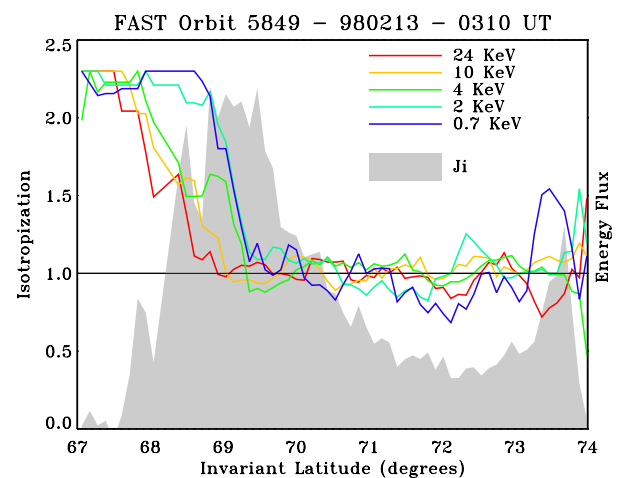


Fig. 5. Isotropy ratios for five ion energies (coloured curves) and the integrated downward energy flux (shaded) for an evening sector auroral oval transit during FAST orbit 5849.

On a given satellite pass through the auroral oval, the dispersion of the IB may not necessarily be consistent with the FLC mechanism. In order to explore this, we identified roughly 1000 northern hemisphere nightside FAST auroral oval transits, and examined the dependence of the latitude of the IB. Figure 6 is a plot of the ion isotropy ratios for energies spanning the 1-25 KeV range for two of those transits. The IB latitude dependence in the two instances is different, one being consistent with, and the other inconsistent with scattering being due to FLC. Of the 1000 transits, roughly 180 of them had IB latitude dependencies that were clearly one way or the other (ie., either higher latitudes corresponding to lower energies, or the reverse). Of those, roughly half were consistent with, and half inconsistent with the FLC mechanism. Figure 7 consists of two histograms illustrating the local time distribution of IB energy dependencies for the two groups.

5 Discussion

Of the FAST auroral transits for which a clear identification of the IB energy dependence was possible, roughly half were

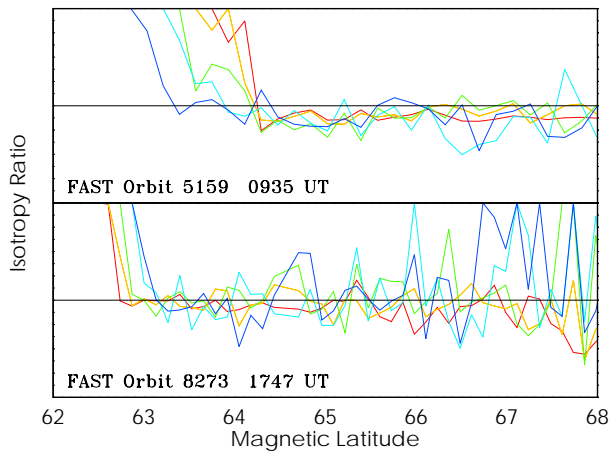


Fig. 6. Isotropy ratios for five energy channels from two FAST auroral oval transits. Red indicates the highest energy channel and blue the lowest.

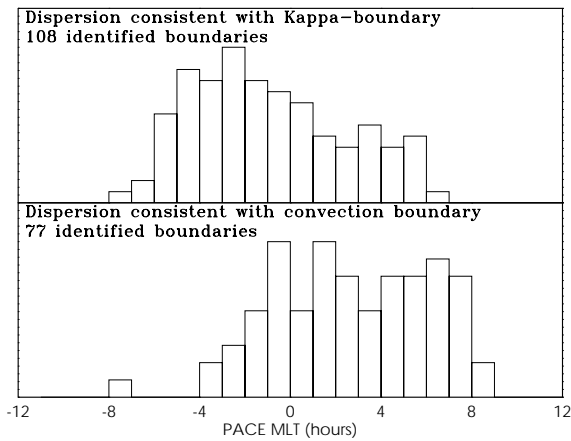


Fig. 7. Local time distribution of IB dispersions that are consistent (top) and inconsistent (bottom) with FLC being the primary cause of strong pitch angle diffusion. See last paragraph in discussion for definition of “convection boundary”.

inconsistent with the FLC scattering mechanism. Furthermore, the MLT distribution of the transits given in Figure 7 shows that the dependence tends to be consistent with, and inconsistent with the FLC mechanism in the evening and morning sectors, respectively.

Identification of IB latitude energy dependencies that are inconsistent with the FLC mechanism, and a local time dependence of the IB latitude energy dependence, are important results. If the scattering does result from FLC, then some additional physical process is occurring at the inner edge of the morning sector CPS which reverses the IB latitude energy dependence. There are a number of possible causes. For example, Kistler et al. (1998) demonstrated that near the inner edge of the morning sector CPS, a consequence of CPS ion charge exchange with the hydrogen geocorona is that a sig-

nificant fraction of the ion population can be He^+ or heavier ions. Our results here are obtained with FAST ESA data, and that instrument does not have mass resolution required to identify this effect. Another possibility is that the drift paths of protons near the inner edge of the CPS lead to anisotropic distribution functions (ie., differential energy fluxes well outside the loss cone larger than those close to the edge of, but outside of, the loss cone) for higher energies (ie., 25 KeV), making what is effectively a larger downgoing loss cone for that energy proton, leading to what we refer to as a convection boundary.

Alternately, the pitch angle scattering that leads to proton auroral precipitation may not be entirely due to FLC. If this turns out to be the case, then these results have important ramifications for the nature and interpretation of the proton aurora. This would, for example, complicate the use of the equatorward boundary of the optical proton aurora as a proxy for the ionospheric projection of the $\kappa=3$ boundary.

We intend to continue this research by exploring processes that might be affecting the ion distribution function in such a way as to produce an IB latitude energy dependence that is inconsistent with FLC causing the pitch angle diffusion. For example, the FAST TEAMS instrument provides mass resolved distribution functions for energies up to 12 KeV (Carlson et al., 1998), and should allow us to determine if the above mentioned charge-exchange process could affect the isotropy ratio in this way.

Acknowledgments

The Gillam MSP is part of the Canadian Space Agency’s CANOPUS array. FAST ESA data was obtained from CDF files publicly available on CDAWeb. We gratefully acknowledge C. Carlson, the PI of the FAST ESA instrument. This research was supported by the Natural Sciences and Engineering Research Council (Canada), through the operating grant of E.D..

References

- Büchner, J., and L. M. Zelenyi, *J. Geophys. Res.*, 92, 13,456, 1987.
- Carlson, C. W., R. F. Pfaff, and J. G. Watzin, *Geophys. Res. Lett.*, 25, 2013, 1998.
- Donovan, E. F., B. J. Jackel, I. O. Voronkov, T. Sotirelis, and N. A. Nicholson, *J. Geophys. Res.*, *accepted*, 2002.
- Imhoff, W. L., J. B. Reagan, and E. E. Gaines, *J. Geophys. Res.*, 82, 5215, 1977.
- Kistler, et. al., *Gephys. Res. Lett.*, 25, 2085, 1998.
- Newell, P. T., Y. I. Feldstein, Y. I. Galperin, and C.-I. Meng, *J. Geophys. Res.*, 101, 10,737, 1996.
- Newell, P. T., V. A. Sergeev, G. R. Bikkuzina, S. Wing, *J. Geophys. Res.*, 103, 4,739, 1998.
- Sergeev, V. A., and N. A. Tsyganenko, *Planet. Space Sci.*, 10, 999, 1982.
- Sergeev, V. A., M. Malkov, and K. Mursula, *J. Geophys. Res.*, 98, 7609, 1993.
- Sergeev, V. A., and B. B. Gvozdevsky, *Ann. Geophys.*, 13, 1093, 1995.
- Wanliss, J. A., J. C. Samson, and E. Friedrich, *J. Geophys. Res.*, 105, 27,673, 2000.